Transactions, SMiRT-23
Manchester, United Kingdom - August 10-14, 2015
Division X

OUT-OF-PLANE SHEAR STRENGTH OF SC WALLS: EFFECTS OF ADDITIONAL FORCES

Kadir C. Sener[1], Amit H. Varma[2] and Saahastaranshu R. Bhardwaj[3]

[1] Research Engineer, Lyles School of Civil Eng., Purdue University, West Lafayette, IN 47906, USA
[2] Professor, Lyles School of Civil Engineering, Purdue University, West Lafayette, IN 47906, USA
[3] Ph.D. student, Lyles School of Civil Engineering, Purdue University, West Lafayette, IN 47906, USA

ABSTRACT

Steel-plate composite walls (SC) are widely used in current nuclear power plant designs. The out-of-plane shear behaviour of SC walls is comparable to that of reinforced concrete (RC) walls. Prior research indicates that the out-of-plane shear strength depends on the contribution of the concrete core (V_c) and the contribution of the steel tie bars (V_s). The out-of-plane shear strength of SC walls has been investigated experimentally and numerically, and the results used to verify corresponding design equations. However, most of this research has been conducted on specimens subjected to monotonic out-of-plane shear loading. This raises concerns regarding the influence of additional forces, particularly, axial tension loading on the out-of-plane shear behaviour of SC walls. These concerns are legitimate because additional forces can cause significant concrete cracking, and compromise its contribution (V_c) to the out-of-plane shear strength.

This paper summarizes the results of experimental investigations conducted on large-scale SC beams to evaluate the effects of axial force, on the out-of-plane shear strength (V_n). The experimental investigations are conducted on large-scale specimens, for which monotonic out-of-plane shear strengths were available for direct comparison. The experimental investigations indicate that axial tension causes significant concrete cracking, but does not limit the out-of-plane shear strength. However, axial tension reduces the flexural capacity (M_n) of the section, and flexural yielding occurs before out-of-plane shear failure as axial tension increases.

INTRODUCTION

Extensive experimental and numerical research programs has been carried out on the out-of-plane shear strength of SC walls by researchers in Japan, S. Korea, China and the US. The experimental database of monotonically loaded out-of-plane shear tests of SC wall beam specimens conducted in different countries is compiled and described in Sener et al. (2014). The experimental database consisted of 39 SC beam specimens with and without shear reinforcement, including a wide range of depths, shear span-to-depth ratios, and longitudinal reinforcement ratios. The study concluded that the behaviour of RC members subjected to out-of-plane shear is similar to that of SC walls. Additionally, the study confirmed the applicability of the ACI code provisions (ACI 349-06) to conservatively estimate the out-of-plane shear strength of SC walls. The ACI code equations were originally developed mainly for reinforced concrete members. The ACI equations to compute the out-of-plane shear strength of reinforced concrete beams in safety related nuclear facilities are given in Equations 1 to 3.

$$V_n = V_c + V_s \tag{1}$$

$$V_c = 2\sqrt{f'_c}A_c \tag{2}$$

$$V_s = A_v f_{yt} \frac{d}{S} \quad (3)$$

In Equation 1; V_n is the nominal out-of-shear strength of the member which is the summation of contributions from the concrete infill (V_c) and shear reinforcement (V_s). In Equation 2, the concrete shear strength contribution (V_c) is a function of the concrete compressive strength (f'_c) and the effective cross sectional area of concrete (A_c). In Equation 3, the shear reinforcement contribution (V_s) is a function of the cross section area of shear reinforcement (A_v), yield strength of the shear reinforcement (f_{yt}), depth of the section (d) and spacing of the shear reinforcement (S).

Limited experimental research has been performed on evaluating the influence of axial tension on shear strength of reinforced concrete beams. The experimental research used to develop code equations indicated significant reduction in the concrete shear strength contribution due to axial tension loading. In this study, experimental tests have been performed in order to determine the effects of axial loading on out-of-plane shear strength and behavior of SC walls. The goal of this paper is to provide recommendations for behavior and design of SC walls subjected to combined axial and out-of-plane shear loading by using the experimental results.

OUT-OF-PLANE SHEAR PLUS TENSION TESTS

The objective of the full-scale tests was to observe the out-of-plane shear behavior of SC walls in the presence of significant axial tension (larger than 500 psi). The concrete shear strength contribution (V_c) is reduced for members subjected significant axial tension according to the ACI code provisions (ACI 349, 2006), as provided in Equation 4. In the equation; N_u is the axial force acting normal to cross section (taken as negative for tension and positive for compression) and A_g is the gross section area. The equation provides a linear reduction in concrete contribution with increasing tension force and neglects the concrete shear strength contribution (V_c) at tensile stress levels in excess of 500 psi. Another objective of this testing was to confirm the applicability of the ACI code out-of-plane shear strength equation to SC design, particularly in regions of high axial tension.

$$V_c = 2(1 + \frac{N_u}{500 A_g})\sqrt{f_c'} A_c \quad (4)$$

Two large-scale tests (OOPV+T-2.0 and OOPV+T-3.5) were conducted to evaluate the effects of axial loading on the out-of-plane shear behaviour and strength of SC walls. The SC beam specimens were tested in a specially designed test setup to apply shear and axial tension loading simultaneously, as shown in Figure 1. The specimens were supported vertically on rotational bearings that were greased to provide smooth sliding/translation. The specimen overhangs were connected to loading beams 1 and 2 using splice plates and through rods. Axial loading is applied using two 1000-kip capacity hydraulic rams that push against the loading columns and beams. This axial force is transferred to the specimen ends through the splice plates and through rods as shown in Figure 1. The out-of-plane loading was applied using a 500-kip capacity hydraulic ram and a special hydraulic setup designed to maintain proportionally increasing tension and out of-plane shear.

Specimen Design and Material Properties

The experimentally tested specimens in this study included similar geometries as the large-scale out-of-plane shear SC wall beam specimens presented in Sener et al. 2014 (SP2 specimens), with the additional axial tensile loading. The steel faceplates were made from ASTM A572 Grade 50 steel. The concrete used for the infill had a nominal compressive strength of 6 ksi, with maximum aggregate size of 38 mm. The

specimens had stud anchors to anchor the steel faceplates to the concrete infill and round deformed rebars for shear reinforcement. The stud anchors and tie bars had identical diameter equal to the faceplate thickness (t_p), but with different spacing (stud spacing, $s=d/4$ and shear reinforcement spacing, $S=d/2$). The specimens had identical section depth, steel faceplate thickness, faceplate reinforcement ratio (ratio of total faceplate area and the wall cross-section area), ρ, of 4.2%, and faceplate slenderness ratio (s/t_p) of 11.3.

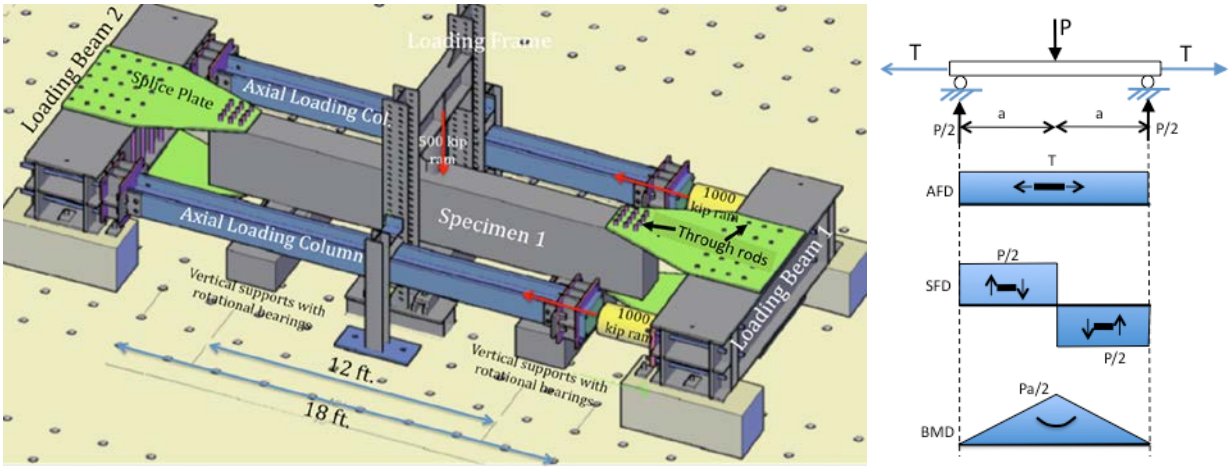

Figure 1. Schematic of setup for subjecting specimens to combined axial tension and out of-plane shear including the corresponding force and moment diagrams

The mechanical properties of the steel faceplates and stud anchors were determined by conducting tests in accordance with ASTM E8 (2003). The average measured yield strength (f_y) and tensile strength (f_u) of the steel faceplates, stud anchors, and shear reinforcement are reported in Table 1 for the tested specimens. The concrete compressive strengths (f'_c) were also measured on the day of test in accordance with ASTM C39 (2014) and are reported in Table 1 for all the specimens.

Table 1: Measured Material Properties of Tested Specimens

Specimen	ASTM A572 Grade 50 Steel Faceplate		A108 Stud Anchors	A496 Tie Bar		Normal weight Concrete	
	Yield Stress (ksi)	Ultimate Stress (ksi)	Yield Stress (ksi)	Yield Stress (ksi)	Ultimate Stress (ksi)	Day of Test Compressive Strength (psi)	Split-Tensile Strength (psi)
OOPV+T-2.0	61.8	79.0	56.2	73.9	93.6	6777	587
OOPV+T-3.5	59.9	86.4	56.2	73.9	93.6	8958	503

Sensor Instrumentation

The instrumentation layout for both specimens was similar. It included electronic pressure transducers to measure the loads applied by the hydraulic rams. These transducers and the hydraulic setup were calibrated using load cells and existing equipment at Bowen Laboratory. The vertical displacements were measured by using displacement transducers at the midspan, along the shear spans, and at the supports. The longitudinal strains in the steel faceplates (both top and bottom) were measured using longitudinal strain gauges at various locations along the length. The specimen end rotations and rotations near the

midspan were measured using rotational transducers (clinometers). Displacement sensors were attached to monitor the change in section depth due to concrete (diagonal tension) cracking induced by the applied shear force. The data from these sensors was used to establish initiation of concrete shear cracking. Concrete cracking was monitored and marked at each load increment during the tests. The crack widths were also measured and noted using crack width gauges.

Testing Approach

The specimens were subjected to: (i) axial loading (T) that is uniform along the length, and (ii) a concentrated out-of-plane load (P) acting at the midspan. The expected axial force, shear force, and bending moment diagrams for the specimens are shown in Figure 1.

OOPV+T-2.0 was subjected to *sequential* loading, with axial loading followed by out-of-plane shear loading. The applied axial tension was equal to 42 percent of the yield strength of the SC section, where the section yield strength is calculated by the total steel faceplate area (A_s) multiplied by the measured yield stress (f_y) of the steel faceplates. The applied axial force corresponded to tension stress of 1.08 ksi over the gross sectional area (T/A_g), which exceeds the stress limit (500 psi) to account for concrete shear strength contribution based on the ACI code equation given in (4). The axial tension loading was maintained constant, while the specimen was subjected to monotonically increasing out-of-plane shear forces up to failure. The specimen shear span ratio-to-depth ratio (a/d) for out-of-plane loading was equal to 2.0.

OOPV+T-3.5 was subjected to *proportionally* increasing axial tension and out-of-plane shear loading. The ratio of the axial tension (T) to out-of-plane force (P) was equal to 3:1. The applied axial tension was equal to 38 percent of the yield strength of the SC section, where the section yield strength is calculated by the total steel faceplate area (A_s) multiplied by the measured yield stress (f_y) of the steel faceplates. The applied axial force corresponded to tension stress of 0.94 ksi over the gross sectional area (T/A_g). The axial loading was maintained constant after reaching this value, and the out-of-plane force was increased either to failure or to the loading capacity of the test setup. The specimen shear span-to-depth ratio (a/d) for out-of-plane loading was equal to 3.5.

The specimens had different section widths, which was *d/2* for OOPV+T-2.0, and *d* for OOPV+T-3.5. Figure 2 shows detailed drawings of both specimens including the stud layouts and spacing in the longitudinal direction and an elevation view of the specimen before casting. The axial loading was transferred to the specimens using through rods at the end sections beyond the vertical supports.

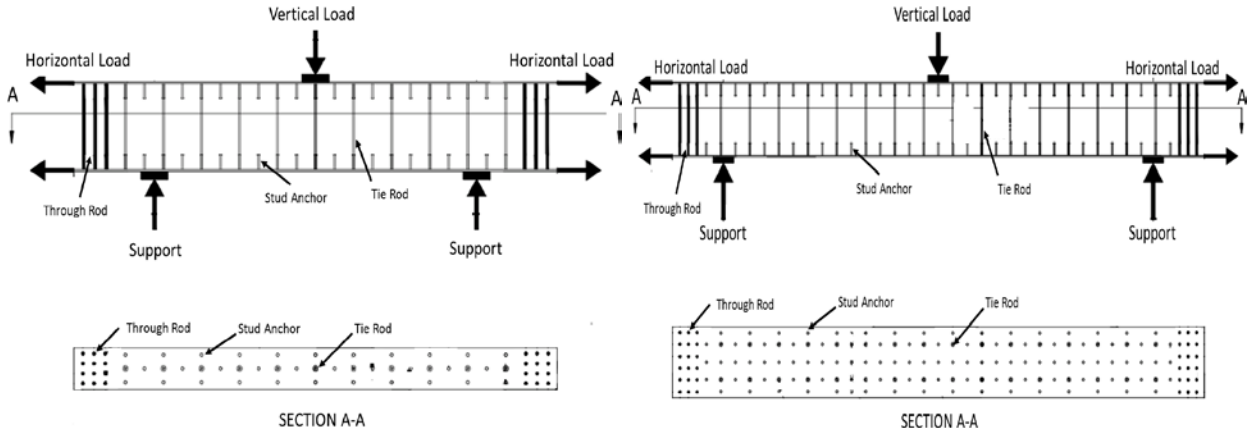

a) OOPV+T-2.0 - sequential loading b) OOPV+T-3.5 - proportional loading

Figure 2. Details of tested specimens

Experimental Results for OOPV+T-2.0

OOPV+T-2.0 was first subjected to an axial tension force of 640 kips and then to vertical shear force. Figure 3 shows the loading protocol for the horizontal (axial tension) and vertical (shear) loading for OOPV+T-2.0. During the axial loading, the specimen developed vertical cracks through the depth of the concrete cross section. The vertical cracks initiated along the length and at the midspan of the specimen at an axial load of 190 kips. The force of 190 kips corresponds to an average concrete stress of 310 psi, which is approximately equal to $4\sqrt{f'_c}$, where the compressive strength f'_c measured on the day of the test. Figure 4 shows a photograph of these vertical cracks along at the midspan of the beam. Additional vertical cracks occurred at axial load levels of 220, 330, and 600 kips. Upon completion of the axial loading, vertical cracks were spaced approximately 6 feet along the length of the specimen.

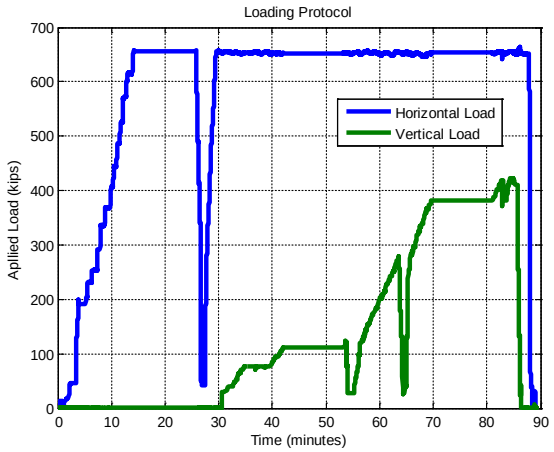

Figure 3. Loading protocol for OOPV+T-2.0

Figure 4. Cracking of OOPV+T-2.0 under axial loading

The measured longitudinal strains in the top and bottom steel faceplates are plotted in Figure 5(a) for different axial force levels. These strain profiles have been developed by connecting the strain gauge measurements on the top and bottom steel faceplates along the beam length for the given load level. The figure shows that the strain levels in the top and bottom faceplates were similar at respective load levels, and reached approximately to 850$\mu\varepsilon$ for axial load of 650 kips. Measuring comparable strain values on the top and bottom faceplates also indicates uniform axial force transfer to the steel faceplates. Converting this strain level to the force resisted by the steel faceplates (850 $\mu\varepsilon$ x E_s x A_s = 630 kips) demonstrates that concrete is not contributing in the axial force resistance of the beam, due to the vertical cracks through the full beam depth observed during the test. The figure indicates nearly-uniform strain distribution along the length, although some non-uniform distribution was observed due to the vertical cracking in concrete (e.g. near midspan).

The axial force was maintained constant while the out-of-plane force was increased monotonically to failure as seen in Figure 3. Figure 5(b) shows the variation of the top and bottom faceplate strains with respect to the out-of-plane shear force. As shown, the out of plane shear force has a small influence on the top faceplate strains, because this region is located closer to the neutral axis for the applied loading combination (tension + shear). Figure 5(b) also indicates that the out-of-plane shear force increased the bottom faceplate strains significantly. The longitudinal strain values measured on the bottom faceplate were largest near the midspan, but both the top and bottom faceplate strains remained less than the yield strain of the steel faceplates of 2131 $\mu\varepsilon$ (measured yield stress = 61.8 ksi).

The measured midspan vertical deflection is shown in Figure 6. The measured shear force-displacement graph indicates that the maximum out-of-plane shear force was equal to 211 kips. Due to the loading configuration, the out-of-plane shear strength was equal to half of the maximum applied vertical load (422 kips/2). The figure also includes horizontal lines representing the calculated contributions of the concrete infill (V_c = 96.6 kips) and steel tie bars (V_s = 78 kips) using Equations 2 and 3 and the measured material properties on the day of the test. The experimental shear strength was greater than both these individual contributions and also their summation ($V_n = V_c + V_s$ = 174.6 kips).

Figure 7 shows a photograph of the inclined shear cracks that formed at 415 kips, prior to the peak load. These inclined shear cracks started from the support location and ended at the load point. The specimen did not have a brittle tie bar failure or fracture at the peak load. The specimen continued to carry the maximum out-of-plane load of 422 kips in spite of the inclined shear crack. The experiment was terminated at this point because the test setup had reached its design capacity. The experimental results indicate that axial tension does not seem to have a significant influence on the out-of-plane shear strength of SC structures.

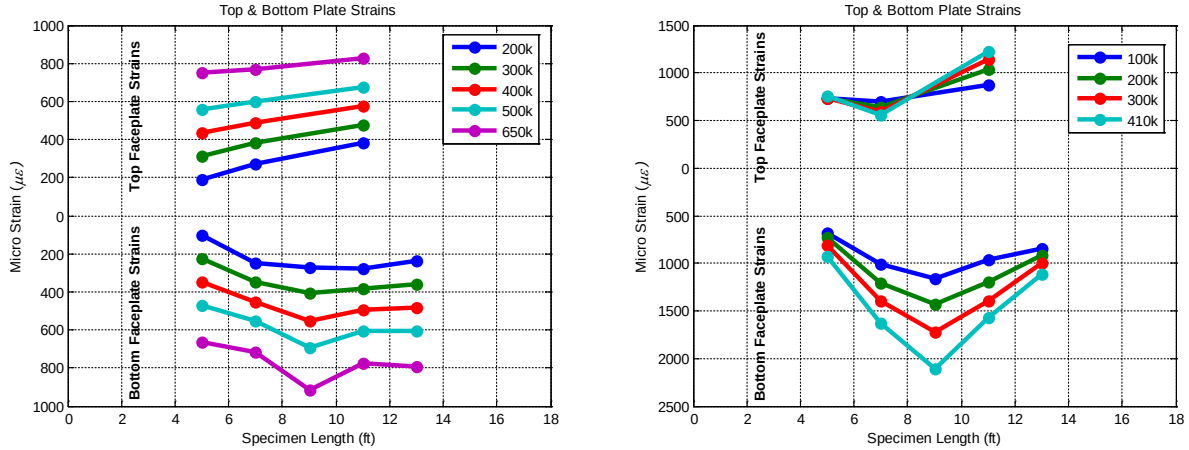

a) b)

Figure 5. Top and bottom steel faceplate longitudinal strain variations with respect to the applied (a) axial and (b) vertical load

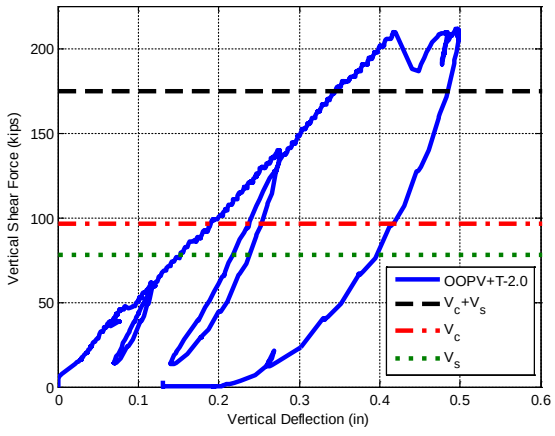

Figure 6. Midspan deflection with respect to vertical shear force

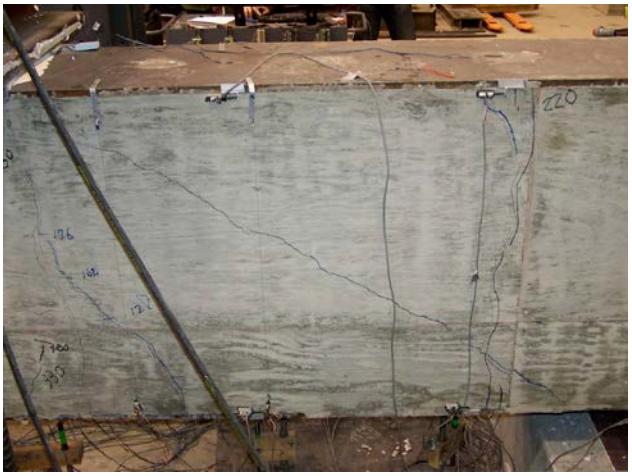

Figure 7. Cracking of OOPV+T-2.0 under shear loading

Experimental Results for OOPV+T-3.5

OOPV+T-3.5 was subjected to proportionally increasing axial tension and out-of-plane loads. Figure 8 shows the loading protocol for the horizontal (axial tension) and vertical (shear) loading for OOPV+T-3.5. The ratio of the proportionally increasing axial tension (T) and out-of-plane forces (P) was approximately equal to 3:1. The maximum applied axial loading was 1150 kips (equal to 38 percent of the measured yield strength of the steel faceplates), and the corresponding out-of-plane load had reached 380 kips. At this point, the applied axial load was maintained constant because the setup reached to the axial force capacity. While the axial load level was constant, the out-of-plane force was increased monotonically from 380 to 550 kips, which was the maximum capacity of the vertical hydraulic ram used for the test.

During the combined horizontal and vertical loading, the specimen initially developed vertical cracks under the load points for applied out-of-plane load of 40 kips. Additional vertical cracks through the depth of the concrete occurred for out-of-plane loads of 80 and 94 kips, as shown in Figure 9. Diagonal shear cracks occurred close to the load point for out of plane load of 234 kips, as shown in Figure 10(a). Diagonal cracks branching from the original vertical cracks occurred for out of plane loads of 251 and 377 kips, as shown in Figure 10(b). However, none of these cracks limited the capacity of OOPV+T-3.5. The specimen continued to carry additional out-of-plane load. The measured tie bar strains remained in the elastic range.

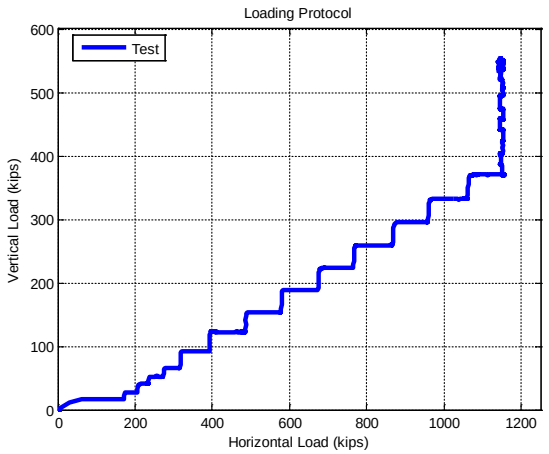

Figure 8. Loading protocol for OOPV+T-3.5

Figure 9. Cracking of OOPV+T-3.5 under combined axial tension and shear loading

The measured longitudinal strains in the top and bottom steel faceplates for different out of plane load levels are plotted in Figure 11. This strain profile has been developed by connecting the strain gauge measurements on the top and bottom steel faceplates along the beam length for the given load level. As shown in Figure 11, the bottom steel faceplate yielded significantly at the midspan, exceeding the yield strain of the steel faceplates of 2066 $\mu\varepsilon$ (measured yield stress = 59.9 ksi). Increasing the vertical load resulted in higher plastic strain levels which led to the flexural yielding failure of the specimen. As shown in Figure 11, some portions of the bottom steel faceplate (between the 5-10 ft region) were still in the elastic region of the response. The figure also shows that the top steel faceplates had small elastic strains which were less than 500 $\mu\varepsilon$. This was due to the top steel faceplate being located closer to the neutral axis for this loading condition and protocol.

a) Shear cracks for out of plane load of 234 kips

b) Shear cracks for out of plane load of 251 kips

Figure 10. Photographs of cracking of OOPV+T-3.5 under combined axial tension and shear loading

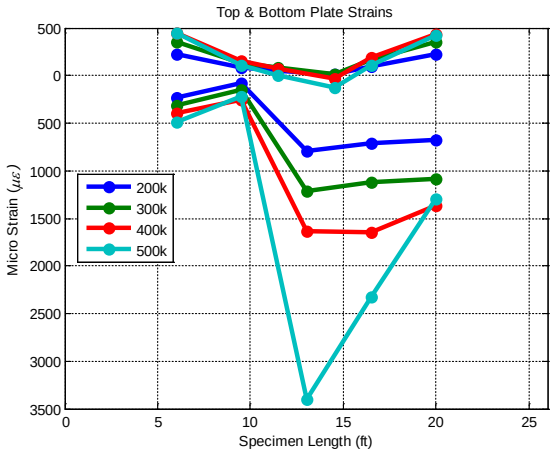

Figure 11. Top and bottom steel faceplate longitudinal strain variations with respect to the vertical load

The measured midspan vertical deflection for OOPV+T-3.5 is shown in Figure 12. The specimen yielded in flexure at an out-of-plane shear force of 250 kips, and midspan deflection of 0.6 inches. As shown in Figure 12, flexural yielding was governed by the yielding of the bottom faceplates. The midspan deflection increased gradually to 1.0 inches and the out of-plane shear force increased to 550 kip. This was the maximum load capacity of the hydraulic ram, and the test was terminated at this point. The specimen is considered to have failed in flexural yielding instead of out-of-plane shear. As explained later, this was the behavior expected from the specimen.

The measured shear force-displacement indicates that the maximum out-of-plane shear force was equal to 277 kips. Due to the three point bending loading configuration, the out-of-plane shear strength was equal to half of the maximum applied vertical load (554 kips/2). The figure also includes horizontal lines representing the calculated contributions of the concrete infill (V_c = 111 kips) and steel tie bars (V_s = 156 kips) using Equations 2 and 3 and the measured material properties on the day of the test. The experimental shear strength was greater than both these individual contributions and also the summation (V_c + V_s = 267 kips). This corroborates the results from the previous specimen that significant axial tension does not seem to have an influence on the out-of-plane shear strength of SC structures.

Figure 13 shows the shear force-midspan displacement comparisons of OOPV+T-3.5 with an identical specimen (SP2a-1, without axial tension force) tested by Sener et al. (2014). The comparison indicates similar initial stiffness but different strength between the specimen, due to OOPV+T-3.5 failing in

flexural yielding before out-of-plane shear failure. Figure 14 shows a panoramic photograph of the overall cracking in OOPV+T-3.5 after the test.

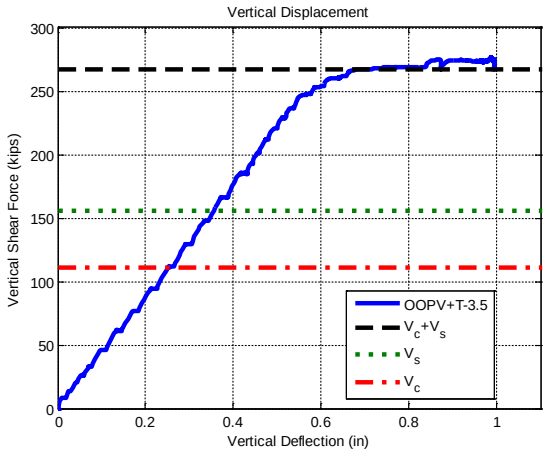

Figure 12. Midspan deflection with respect to vertical shear force

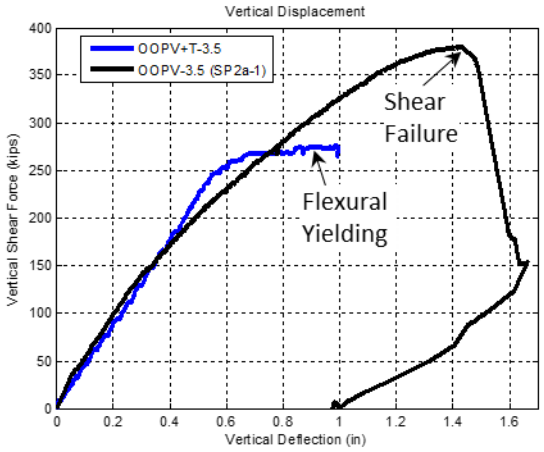

Figure 13. Force-displacement comparison of specimens with & without axial tension load

Figure 14. Cracking map of OOPV+T-3.5 after the test

For OOPV+T-3.5, the midspan moment corresponding to the out-of-plane load was equal to 2887.5 kip-ft. The flexural strength of the specimen for zero axial tension using the measured yield stress was equal to 4124 kip-ft. The strength is based on the flexural strength Equation 5 below, taken from Supplement No.1 to AISC N690-12 [N690s1 (AISC 2014)].

$$M_n = 0.9 A_s f_y d \tag{5}$$

Assuming a linear interaction between axial tension capacity ($A_s f_y$) and the bending moment capacity (M_n), the flexural strength for an applied axial tension of 1150 kips (38% of $A_s f_y$), can be estimated as 62% of the flexural strength M_n with no axial loads (i.e., 0.62 x 4124 = 2557 kip-ft). As shown, the moment capacity (2887.5 kip-ft) of OOPV+T-3.5 was 13 percent higher than that estimated flexural strength (2557 kip-ft). This was probably because of the tension stiffening effect of concrete, rotational restraints at the ends, and steel overstrength due to hardening of the steel faceplates.

CONCLUSIONS AND RECOMMENDATIONS

This paper summarizes the results of experimental investigations conducted on large-scale steel-plate composite wall (SC) beams to evaluate the effects of axial force, on the out-of-plane shear strength (V_n). Two large-scale tests were conducted on SC specimens subjected to combined axial tension and out of plane shear. The first specimen (OOPV+T-2.0) with shear span-to-depth ratio (a/d) of 2.0 was subjected to axial tension followed by out-of-plane shear loading. The second specimen (OOPV+T-3.5) with shear span-to-depth ratio (a/d) of 3.5 was subjected to proportionally increasing axial tension and out-of-plane shear loading. The test results demonstrated that even in the presence of significant axial tension, the out-of-plane shear strength could be calculated conservatively using the ACI 349 code provisions for RC beams without considering the effects of axial tension.

The experimental results for OOPV+T-3.5 indicated that the axial tension reduces the flexural strength. The experimental response of OOPV+T-3.5 was compared to an identical specimen tested without axial tension and similar behaviour was observed. However, the out-of-plane load capacity of OOPV+T-3.5 was reduced due to flexural yielding. The flexural strength of specimen subjected to axial tension was accurately calculated using a linear interaction between the axial tension and bending moment capacities.

ACKNOWLEDGMENTS

The research presented in this paper was funded partially by Purdue University. The authors thank Mr. Tom Bradt and Dr. Jungil Seo for their assistance in conducting the tests at Bowen Laboratory.

REFERENCES

ACI 349-06 (2006). *Code Requirements for Nuclear Safety-Related Concrete Structures and Commentary.* American Concrete Institute, Farmington Hills, MI.

American Institute of Steel Construction (2014). *Specification for Safety-Related Steel Structures for Nuclear Facilities Supplement No. 1*. AISC N690s1. PUBLIC REVIEW DRAFT DATED 5-1-14. American Institute of Steel Construction, Chicago, IL.

ASTM Standard C39. Specification for concrete aggregates. ASTM International, West Conshohocken, PA, 2003. www.astm.org

ASTM Standard E8. *Standard test methods for tension testing of metallic materials*. ASTM International, West Conshohocken, PA, 2003. www.astm.org

Sener, K., and Varma, A.H. (2014). "Steel-Plate Composite SC Walls: Experimental Database and Design for Out-of-Plane Shear." *Journal of Constructional Steel Research*, Elsevier Science, Vol. 100, pp. 197-210, http://dx.doi.org/10.1016/j.jcsr.2014.04.014